J Mater Sci (2010) 45:3102–3105
DOI 10.1007/s10853-010-4298-6

LETTER

Influence of morphology and processing on XPS characterisation of SrO–Ca–ZnO–SiO_2 glass

F. R. Laffir · A. W. Wren · M. R. Towler

Received: 12 August 2009 / Accepted: 3 February 2010 / Published online: 18 March 2010

X-ray Photoelectron Spectroscopy (XPS) has proven and continues to be a useful technique in the characterisation of alkali silicates, alkaline earth silicates, and other novel forms of bioactive glass [1–3]. Binding energy of O 1s electrons is revealing of the role played by cations introduced into a glass network and thus helps to establish the reactivity of different glass formulations [4]. Bridging (BO) and non-bridging oxygens (NBO) corresponding to network formers/modifiers can be distinguished in most cases [3–6]. Network modifiers provoke the disruption of the continuity of the glass network due to the breaking of Si–O–Si bonds [7] with the resulting NBO appearing at a lower binding energy. Hence, the study of the bonding configuration of glasses and the identification of the Si–O–NBO groups by analytical techniques, such as XPS, can contribute to improving the ability to design new glass formulations [7].

XPS is a surface sensitive technique and contaminants on the surface can have undesirable effects on measurements. A glass surface exposed to air can minimise high energy surface sites by adsorbing molecules from the atmosphere with the kinetics of the process depending on the glass composition and thermal processing of the surface [8]. Oxygens from adsorbed molecules such as H_2O, CO, CO_2, and hydrocarbon species contribute to the O 1s peak and can interfere in the evaluation of BO and NBO content in glass. In order to minimise contamination, glass specimens are generally cleaved in ultra high vacuum giving rise to pristine surfaces.

The glass formulation under investigation here was originally synthesised for the purpose of developing a novel glass polyalkenoate cement (GPC) [9, 10]. In a recent study by the authors [2], XPS was used to characterise the glass phase of one of these glasses (BT101—$4SrO{\cdot}12CaO{\cdot}36ZnO{\cdot}48SiO_2$) in its powdered form. In this letter, however, XPS is used to characterise the same glass formulation produced by the traditional melt quench route (G_{Melt}) described in detail elsewhere [9, 10] and compared with samples produced in glass rod form. BT 101 rod was produced by weighing out appropriate quantities of analytical grade reagents (Sigma–Aldrich, Dublin, Ireland) and firing in a platinum crucible (1480 °C, 1 h). In a separate furnace, a graphite mould was placed at T_g-20 °C and was filled with the glass melt and held at this temperature for 1 h before furnace cooling. Glass rods were cut and shaped into approximate dimensions of 15 × 3 × 3 mm^3.

XPS was performed using a Kratos AXIS 165 spectrometer. A monochromatic Al Kα radiation source ($h\upsilon = 1486.6$ eV) at a fixed pass energy of 20 eV was used. All spectra were calibrated using C 1s of adventitious carbon as a reference. Surface charge was efficiently neutralised by flooding the sample surface with low energy electrons. The glass rod was fractured (G_{Frac}) in the treatment chamber (2×10^{-8} torr) and transferred immediately into the analysis chamber where the pressure was maintained at $\sim 2 \times 10^{-9}$ torr. This fractured surface was then exposed (G_{Exp}) in air for 10 days and analysed, and then ground to a powder (G_{Pow}) for further analysis. For peak synthesis of high resolution spectra, a mixed Gaussian-Lorenzian function with a Shirley type background subtraction was used. Average data from duplicate analyses are quoted with an uncertainty of less than ± 1%, except

F. R. Laffir
Materials and Surface Science Institute,
University of Limerick, Limerick, Ireland

A. W. Wren (✉) · M. R. Towler
Inamori School of Engineering, Alfred University,
Alfred, NY 14802, USA
e-mail: wren@alfred.edu

Table 1 Relative percentage atomic concentration of modifiers (M = Zn, Ca, Sr) and Si of BT101 glass in its different forms

Glass form	Zn	Ca	Sr	Si	Si/M
G_{Melt}	17.4	9.4	5.1	68.0	2.1
G_{Frac}	23.3	13.6	5.4	57.7	1.4
G_{Exp}	19.4	13.1	6.0	61.5	1.6
G_{Pow}	19.6	13.2	5.7	61.5	1.6

for C and O concentrations of powder and exposed fractured surface which were better than ± 2.5%. For O 1s photoelectron peaks which are not well resolved, choice of initial fitting parameters can affect the uncertainty in evaluating NBO and BO components.

High resolution photoelectron spectra of Zn 2p, Ca 2p, Sr 3d, Si 2p, O 1s, and C 1s were recorded for the different forms of glass. The relative atomic concentrations of Zn, Ca, Sr (collectively classed as M), and Si are presented in Table 1. Zn, Ca, and Sr are believed to act as modifier cations in the glass network [11].

It is evident from Table 1 that there is a significant difference in the concentration of cations detected, in particular between G_{Melt} and G_{Frac}. The ratio of Si:M was found to be much higher for G_{Melt} (2.1) as compared to G_{Frac} (1.4), G_{Exp} (1.6) and G_{Pow} (1.6) and this is likely due to the G_{Melt} sample being shock quenched in water. An aqueous environment acts as a medium where ions present on a glass surface will migrate. Also, the glass frit produced during G_{Melt} has a much higher surface area which will enhance ion migration. An increase in Zn^{2+} and Ca^{2+} is observed for the G_{Frac} surface and is generally higher in other forms produced by the glass rod route (G_{Exp} and G_{Pow}). When G_{Frac} surface is left in air, the Si:M ratio decreases and reaches that of G_{Pow}. It is apparent there is a significant contribution from the processing history of powder and rods, whilst they are made of the same formulation.

Figures 1 and 2 show the O 1s spectrum for G_{Frac} and G_{Melt}, respectively. The O 1s spectrum for G_{Frac} surface is a single peak, however, the asymmetry and full width half maximum (FWHM) of 2.1 eV indicate the existence of two component peaks. Since there is no evidence of hydrocarbon contaminants containing oxygen from the C 1s spectrum on the vacuum cleaved surface (Fig. 3); the oxygen peak can be resolved confidently into two components to represent BOs and NBOs. The asymmetry is on the higher binding energy region, therefore the NBOs can be selected first to conform to the steep right side of the peak and allow the data processing software (CasaXPS) freedom to fit the rest of the spectrum with a second component peak belonging to BOs. The % area under the curves labelled BO and NBO agrees well with theoretically

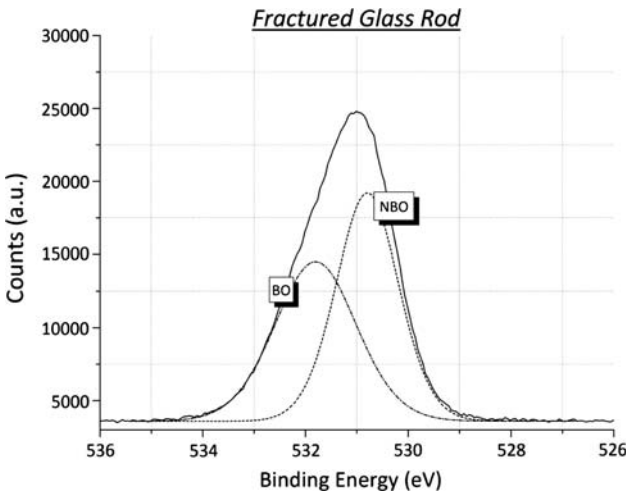

Fig. 1 High resolution O 1s spectrum of vacuum G_{Frac} rod

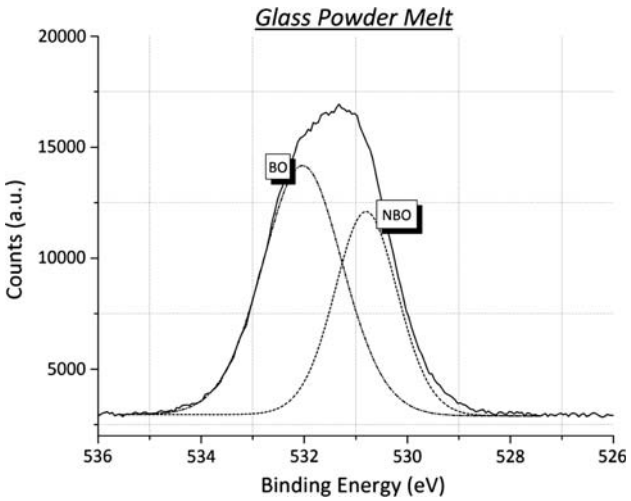

Fig. 2 High resolution O 1s photoelectron spectrum of G_{Melt}

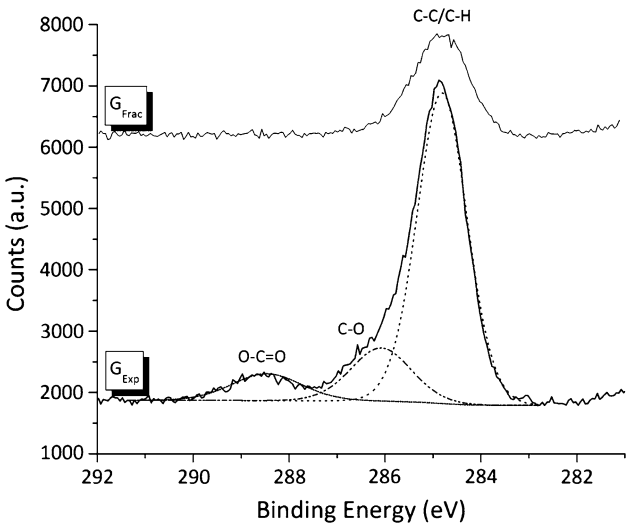

Fig. 3 High resolution C 1s photoelectron spectrum

Table 2 Binding energy (eV), FWHM (eV), and the experimental (corrected) and calculated percentage of NBOs and BOs in the different forms of the BT101 glass

Glass form	Binding energy (eV)	FWHM (eV)	Corrected/ calculated area %	Ratio NBO/BO
G_{Melt}	530.8	1.44	40.8 ± 0.7 (39.7)	0.69
	532.0	1.83	59.2 ± 0.7 (60.3)	
G_{Frac}	530.8	1.44	52.2 ± 0.6 (53.8)	1.09
	531.8	1.87	47.8 ± 0.6 (46.2)	
G_{Exp}	530.6	1.44	48.5 ± 0.8 (47.7)	0.94
	531.6	1.95	51.5 ± 0.8 (52.3)	
G_{Pow}	530.8	1.44	48.9 ± 0.6 (47.2)	0.95
	532.0	1.81	51.1 ± 0.6 (52.8)	

calculated values shown in Table 2, using the Eq. 1 which gives the fraction of NBOs [12]. Uncertainty in the % area measured from BO and NBO peaks is less than ± 1%.

$$\frac{\text{NBO}}{O_T} = \frac{2 \times \text{mol}\%M}{\text{mol}\%M + (2 \times \text{mol}\%\text{SiO}_2)} \quad (1)$$

This equation is based on the condition that every M^{2+} ion has two neighbouring NBOs. Mol% M and mol% SiO_2 correspond to the total concentration of modifiers (Zn, Ca, and Sr) and Si in the glass as determined by quantitative XPS given in Table 1. O_T is the total oxygen content which is equal to one oxygen in each mol% of M and two oxygens in each mol% of SiO_2.

NBOs can arise from similar chemical environments in different physical forms of the same glass formulation BT101; therefore, FWHM and binding energy of the NBO component of the different forms of glass are constrained to that of the G_{Frac} rod. O 1s spectrum for G_{Melt} shown in Fig. 2 is more symmetrical and has a FWHM of 2.5 eV. The related C 1s spectrum shows the presence of C–O and carboxyl groups with the corresponding oxygens appearing at binding energies of ~532 eV [13]. This contribution can be subtracted from BO component and the corrected percentage composition of NBOs and BOs is presented in Table 2. Error in the measurement of FWHM of the BO peak is less than ± 0.8 eV. There is good agreement with those calculated from modifier and Si compositions obtained from Table 1 using Eq. 1. Table 2 also illustrates the ratio of BO/NBO for each sample. It is evident that the G_{Melt} sample has a much lower ratio of BO/NBO (0.69) as compared to each of the glass rod samples, G_{Frac} (1.09), G_{Exp} (0.94), and G_{Pow} (0.95). Again this is likely due to the production route where the bulk glass that is cooled slowly in a furnace retains more cations, predominantly Zn^{2+} than the glass melt quench route where cations are leached into water during cooling.

When the G_{Frac} surface is left exposed to air (G_{Exp}), species containing C–O (286.2 eV) and carboxyl (288.8 eV) groups start to develop as observed from the C 1s spectrum shown in Fig. 3. It is also evident that there is a reduction in the ratio of BO/NBO with G_{Exp} and G_{Pow} as compared to G_{Frac}. In the study of alkali tellurite glasses by Himei et al. [14], O 1s peak of glass exposed in atmosphere had a higher binding energy component absent from vacuum fractured glass which was later assigned to oxygen in contaminant carbonates and hydroxides. Since the oxygens can be accounted for within an uncertainty of ± 1.7%, it is likely there is no significant adsorption of water/hydroxyls from moisture in the atmosphere and BT101 glass may be less hygroscopic than other glass formulations.

It is also interesting to note that there is an enrichment of Zn^{2+} at the surface of G_{Frac} in conjunction with a corresponding decrease in Si concentration (57.7%) compared to G_{Exp} (61.5%) and G_{Powd} (61.5%). This phenomenon is supported by studies on alkali silicate glasses where Na^+ [15, 16] and K^+ [17, 18] enrich the surface of a fractured glass. Molecular simulation studies of SiO_2–Na glasses have shown that upon cleaving a surface, there is a spontaneous migration of Na^+ ions to the surface region accompanied by NBOs [19]. Similar studies on SiO_2–Al–Ca–Na glasses show, in addition to Na^+ being the dominant migrant, evidence for migration of Ca^{2+} ions [16]. A lower surface free energy environment drives the migration of network modifiers while the network formers such as Si and Al remain evenly distributed. Size and valency effects in the phenomenon of surface enrichment are not yet fully understood. In this study of BT101 glass, there is preferential enrichment of Zn^{2+} with an increase in the proportion of NBO. The relative atomic concentration of Zn in BT101 glass is high and can give rise to a steeper diffusion gradient. Furthermore, Zn^{+2} divalent cation is small (74 pm) compared to Ca^{+2} (99 pm) or Sr^{+2} (141 pm) and suggests that smaller cations have preference to migrate and enrich the surface. As the cleaved surface is left in air, adsorption of molecules from the atmosphere disturbs the surface equilibrium dynamics resulting in a decrease in the modifier cation concentrations. Quadrupole mass spectroscopy and surface ionization studies [15] have measured atomic Na emission accompanying fracture of sodium trisilicate glass and emission peaks at 3–6 ms after a fracture

event and decay over tens of milliseconds. It may be that Zn^{2+} ions are liberated after fracture when left exposed revealing more of the underlying Si groups. Understanding of this phenomenon is beyond the scope of this study and will be explored further by other theoretical and experimental investigations.

In this letter, XPS measurements highlight the differences in the surface composition of BT101 glass produced from different processing routes, namely powder and rods and also the effect of exposure to contaminants from the surrounding atmosphere. Vacuum cleaved surface measures an appreciable increase in modifier cations. This may have implications when evaluating accompanying BO and NBO content of glass. However, further studies on different glass formulations with different size and valency cations will be essential to understand the mechanism of cation enrichment on vacuum cleaved glass surfaces.

References

1. Roy B, Jain H, Saha SK, Chakravoryt D (1995) J Non-Cryst Solids 183:268
2. Wren AW, Clarkin OC, Laffir FR, Ohtsuki C, Kim IY, Towler MR (2009) J Mater Sci Mater Med 20(10):1991
3. Mekki A, Salim J (1999) J Electron Spectros Relat Phenomena 227:101
4. Dalby KN, Nesbitt HW, Zakaznova-Herzog VP, King PL (2007) Geochim Cosmochim Acta 71:4297
5. Roy B, Jain H, Saha SK, Chakravorty D (1998) J Am Ceram Soc 81:2360
6. Soares PC, Nascente PAP, Zanotto ED (2002) Eur J Glass Sci Tech Part B 43:143
7. Serra J, Gonzalez P, Liste S, Serra C, Chiussi S, Leon B, Perez-Amor M, Ylanen HO, Hupa M (2003) J Non-Cryst Solids 332(1):20
8. Pantano CG (1985) Strength of inorganic glass. Plenum Publishing Corporation, New York
9. Wren AW, Boyd D, Towler MR (2008) J Mater Sci Mater Med 19:1737
10. Boyd D, Wren AW, Clarkin OM, Towler MR (2008) J Mater Sci Mater Med 19(4):1745
11. Boyd D, Watts S, Hill RG, Wren AW, Clarkin OM, Towler MR (2008) J Mater Sci Mater Med 19:953
12. Shelby JE (2005) An introduction to glass science and technology. Royal Society of Chemistry, Cambridge
13. Briggs D, Seah MP (1990) Practical surface analysis. John Wiley, London
14. Himei Y, Miura Y, Nanba T, Osaka A (1997) J Non-Cryst Solids 211(1):64
15. Langford SC, Jensen LC, Dickinson JT, Pederson LR (1991) J Mater Res 6:1358
16. Corrales LR, Du J (2006) J Am Ceram Soc 89:36
17. Gedeon O, Zemiek J (2003) J Non-Cryst Solids 320:177
18. Zemek J, Jiricek P, Gedeon O, Lesiak B, Jozwik A (2005) J Non-Cryst Solids 351:1665
19. Abbas A, Delaye JM, Ghaleb D, Calas G (2003) J Non-Cryst Solids 315:187